

# The Superconducting Critical Temperature

Mike Guidry<sup>1,a</sup>, Yang Sun<sup>2,b</sup>, and Lian-Ao Wu<sup>3,c</sup>

<sup>1</sup> Department of Physics and Astronomy, University of Tennessee, Knoxville TN 37996, USA

<sup>2</sup> School of Physics and Astronomy, Shanghai Jiao Tong University, Shanghai 200240, People's Republic of China

<sup>3</sup> IKERBASQUE, Basque Foundation for Science, 48011 Bilbao, Spain, and Department of Theoretical Physics and History of Science, Basque Country University (EHU/UPV), Post Office Box 644, 48080 Bilbao, Spain

**Abstract.** Two principles govern the critical temperature for superconducting transitions: (1) intrinsic strength of the pair coupling and (2) effect of the many-body environment on the efficiency of that coupling. Most discussions take into account only the first but we argue that the properties of unconventional superconductors are governed more often by the second, through dynamical symmetry relating normal and superconducting states. Differentiating these effects is essential to charting a path to the highest-temperature superconductors.

## 1 Introduction

Conventional superconductivity (SC) is described well by BCS theory using spherical ( $s$ -wave) pairing formfactors corresponding to phonon pair binding. Superconductors with formfactors that are not  $s$ -wave are termed *unconventional*; the most famous are cuprate high-temperature superconductors, which have  $d$ -wave pairing and high transition temperatures  $T_c$  relative to conventional SC. Many other unconventional superconductors are known, often exhibiting  $T_c$  larger than for conventional SC. Superconductors involve Cooper-pair condensates and stronger pairing favors survival of the condensate at higher  $T$ . Thus, enhancing phonon coupling by tuning atomic mass and lattice spacing can increase  $T_c$  for conventional SC. For unconventional SC the situation is more nuanced. The value of  $T_c$  depends on intrinsic pairing strength (through electron correlations rather than phonons), but there is another factor, often more important and often overlooked in standard discussions. This is seen most clearly by viewing the SC transition from the perspective of *fermion dynamical symmetry*.

## 2 Fermion Dynamical Symmetry and Superconductivity

The fermion dynamical symmetry method uses principles of dynamical symmetry to truncate a Hilbert space to a collective subspace, specified in terms of a Lie algebra having a relatively small number of fermionic generators, as illustrated in Fig. 1(a). Within the subspace the most general Hamiltonian is a polynomial in the Casimir invariants for all the subgroup chains of

---

<sup>a</sup> e-mail: [guidry@utk.edu](mailto:guidry@utk.edu)

<sup>b</sup> e-mail: [sunyang@sjtu.edu.cn](mailto:sunyang@sjtu.edu.cn)

<sup>c</sup> e-mail: [lianaowu@gmail.com](mailto:lianaowu@gmail.com)

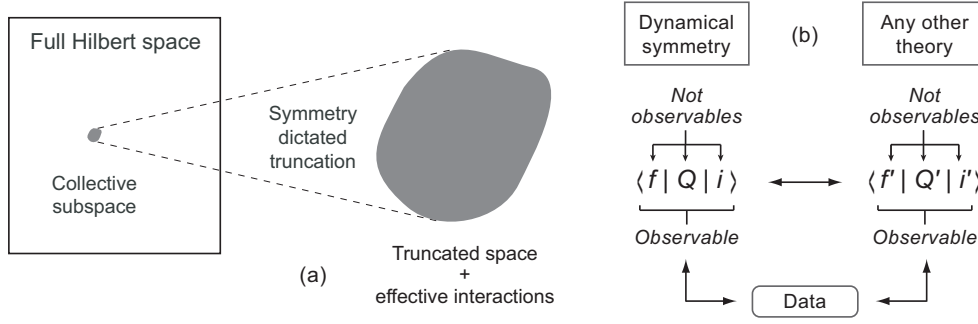


**Fig. 1.** (a) Emergent-symmetry truncation of Hilbert space to a collective subspace using principles of dynamical symmetry. (b) Comparison of matrix elements among different theories and data. Wavefunctions and operators are *not observables*. Only matrix elements are directly related to observables.

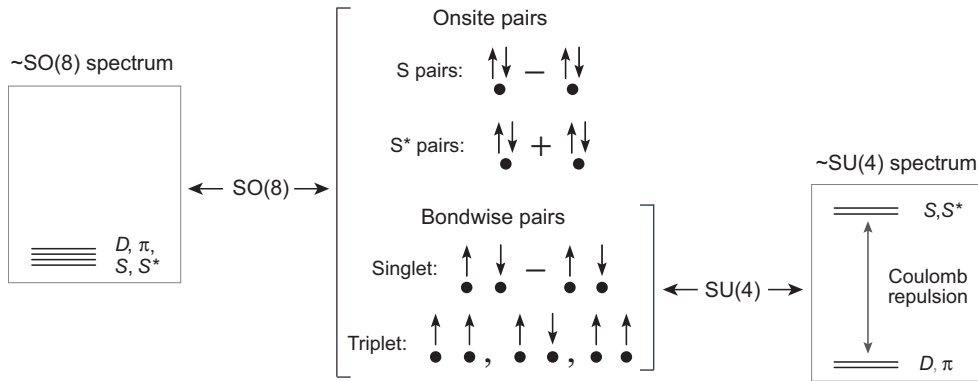


**Fig. 2.** Schematic difference between bondwise ( $D, \pi$ ) and onsite ( $S, S^*$ ) pair energies. If onsite repulsion is weak the pairing states are nearly degenerate, yielding an  $SO(8)$  symmetry. If it is strong onsite pairs are pushed up in energy, reducing the symmetry to an effective  $SU(4)$  low-energy symmetry.

the highest symmetry consistent with conservation laws, with coefficients of the terms determined by effective interactions representing the average effects of the space excluded by the truncation. Matrix elements can be determined exactly in specific limits and approximately using coherent state methods otherwise. As illustrated in Fig. 1(b), the theory is *microscopic* because the only valid comparison in quantum mechanics is for matrix elements.

A description of cuprate superconductors by this method is outlined in Figs. 2 and 3. Restricting to the 28 generators describing onsite and nearest-neighbor pairing, antiferromagnetic, spin, and charge degrees of freedom, the minimal symmetry is  $SO(8)$ . If Coulomb repulsion is weak and antiferromagnetic (AF) correlations are negligible, onsite pairs are favored over bondwise pairs (for simplicity we restrict to nearest-neighbor bondwise pairs here). This favors subgroup chains containing  $SU(2)$  pseudospin generators that give conventional SC described by  $SU(2)_{\text{BCS}}$  symmetry. If Coulomb repulsion is strong and antiferromagnetism significant, onsite pairing is disfavored relative to bondwise pairing and antiferromagnetic operators become important in addition to pairing operators. This reduces  $SO(8)$  to a 15-generator subgroup  $SU(4)$ , with generators representing AF, spin-singlet and spin-triplet bondwise pairs, spin, and charge operators; explicit forms for the operators and their commutation relations are given in Refs. [1, 11]. Three dynamical symmetry chains have exact solutions and correspond (through their matrix elements) to physical states thought to be relevant for cuprate doped and undoped states:

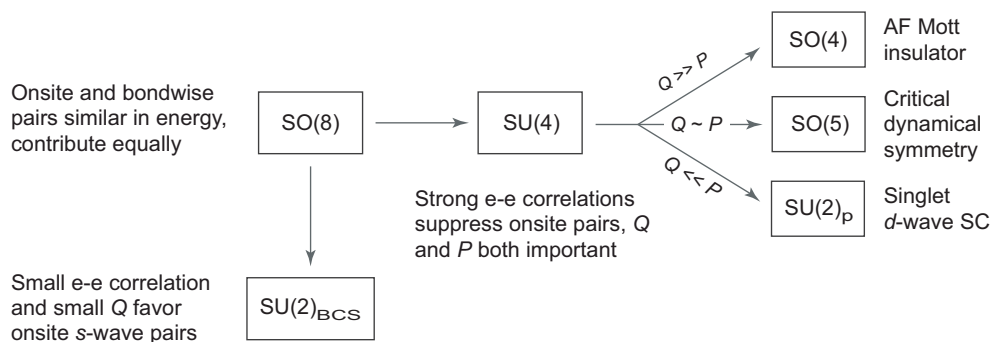


**Fig. 3.** The relationship between SO(4), SO(8), and BCS SU(2) symmetry for conventional and unconventional superconductors.

1.  $SU(4) \supset SO(4)$ , which represents an antiferromagnetic (AF) Mott insulating state that is the low-temperature ground state for zero doping.
2.  $SU(4) \supset SU(2)$ , which represents a  $d$ -wave singlet superconducting (SC) state that can become the low-temperature ground state for non-zero doping.
3.  $SU(4) \supset SO(5)$ , which represents a critical dynamical symmetry interpolating between the SU(2) superconducting and SO(4) antiferromagnetic solutions.

We will now document concisely in Section 3 that this microscopic approach gives a remarkably good description of a broad range of cuprate phenomena with minimal assumptions, and then use the validated SU(4) theory to discuss SC transition temperatures in Section 4.

### 3 SU(4) Dynamical Symmetry and Cuprate Phenomenology

The properties of high-temperature superconductors (HTSC) raise fundamental questions that have proven difficult to answer in a comprehensive way: (1) What physics controls the phase diagram? (2) What role do quantum phase transitions (QFT) and quantum critical behavior play, and what is their microscopic origin? (3) How does the Cooper instability arise in a doped Mott insulator? (4) What is the origin of the pseudogap (PG), and do “competing order” or “preformed pairs” govern its properties; how is the PG related to the AF and SC phases? (5) Why do underdoped cuprates exhibit complexity and disorder despite a highly universal overall phase diagram? (6) How are HTSC (and other unconventional superconductors) related to conventional SC? (7) Why is  $T_c$  higher than expected for unconventional superconductors? (8) What principles can guide searches for new high- $T_c$  superconductors? (9) How is HTSC related to the various forms of SC and superfluidity that occur in other fields of physics? In our opinion, no standard approach can provide plausible answers to this entire list without ad hoc assumptions. Let us now apply the the SU(4) model of HTSC to answering the questions posed above. The model is documented in a series of publications [1, 2, 3, 4, 5, 6, 7, 8, 9, 10] and a comprehensive review [11]. Here we collect in one place a unified set of physical implications for SU(4) symmetry, unobscured by technical detail. Hence, we shall write few equations, preferring to emphasize physical interpretation and referencing the literature where ample equations, derivations, and technical justification may be found.

**Origin of the Phase Diagram:** Universality of the cuprate phase diagram suggests a unifying principle independent of microscopic details. The SU(4) model implies that symmetry alone dictates many basic properties, and that these properties lead to a highly universal phase diagram, illustrated in Fig. 4, that is described quantitatively by the SU(4) model. Only two significant parameters enter: the effective strength of singlet pairing  $G_0$  and the effective

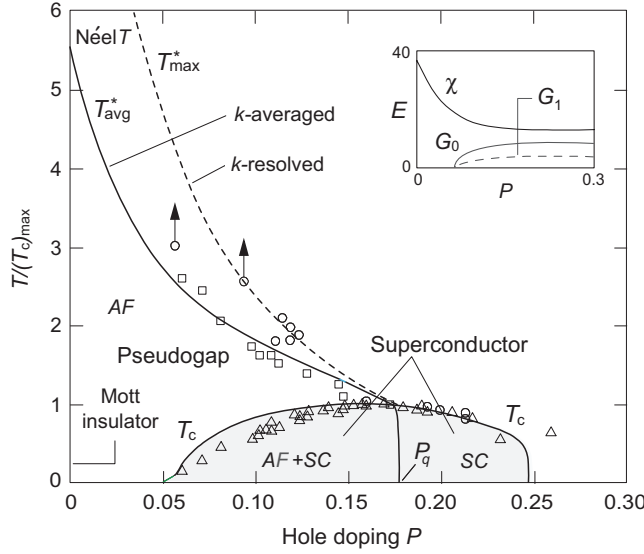


**Fig. 4.** SU(4) cuprate temperature  $T$  and doping  $P$  phase diagram compared with data taken from Refs. [12, 13]. Strengths of the AF and singlet pairing correlations were determined in Ref. [5] by global fits to cuprate data (inset plot). Pseudogap temperatures are indicated by  $T^*$ . The two PG curves correspond to whether momentum is resolved or not in the experiment. The inset shows the variation of the AF and pairing coupling with doping  $P$ .

strength of AF correlations  $\chi$  (triplet pairing strength  $G_1$  has minimal influence). The best fit is for the smooth dependence of  $G_0$  and  $\chi$  on the doping  $P$  shown in the inset of Fig. 4, but the basic features survive if these parameters are held constant with doping (see Ref. [11]). Thus *the cuprate phase diagram is a consequence of SU(4) symmetry correlating emergent  $d$ -wave singlet pairing and antiferromagnetism; it depends only parametrically microscopic details such as pairing formfactors.*

**AF Mott Insulator States at Half Filling:** By counting, SU(4) symmetry requires *no double occupancy of lattice sites* by correlated fermions [3]. Hence, charge transport is suppressed at half band-filling and the undoped ground state is a *Mott insulator*. Moreover, this state has  $SU(4) \supset SO(4)$  dynamical symmetry and the matrix elements of an AF Néel state [1, 2, 11]. Thus, the undoped SU(4) ground state is an *AF Mott insulator*, just as observed for cuprates.

**Cooper Instability of the Doped Mott Insulator:** The same SU(4) symmetry requiring the undoped ground state to be an AF Mott insulator implies that this state is *fundamentally unstable against condensing Cooper pairs* when doped [9, 11]. This results in a quantum phase transition (QPT) to be discussed more extensively below, and implies a rapid transition to a superconducting state upon doping, as observed for data in Fig. 4.

**Upper Doping Limit for Superconductivity:** Direct counting implies that occupancy of more than  $\frac{1}{4}$  of lattice sites by holes will break SU(4) and destroy SC [1, 3]. This is in accord with the data displayed in Fig. 4, where  $T_c > 0$  only for doping less than  $\sim 25\%$  holes.

**Optimal Doping for Superconductivity:** For doping larger than that near the peak of the superconducting dome (optimal doping) in Fig. 4, SC properties are observed to become better defined. As discussed further below, this is a natural consequence of SU(4) symmetry, which implies a quantum phase transition near optimal doping exhibiting critical behavior [11]. At subcritical doping the superconducting wavefunction is perturbed by residual AF correlations. At the QFT the AF correlations vanish identically, leaving pure  $d$ -wave, BCS-like, singlet SC above critical doping. This is consistent with various cuprate experiments.

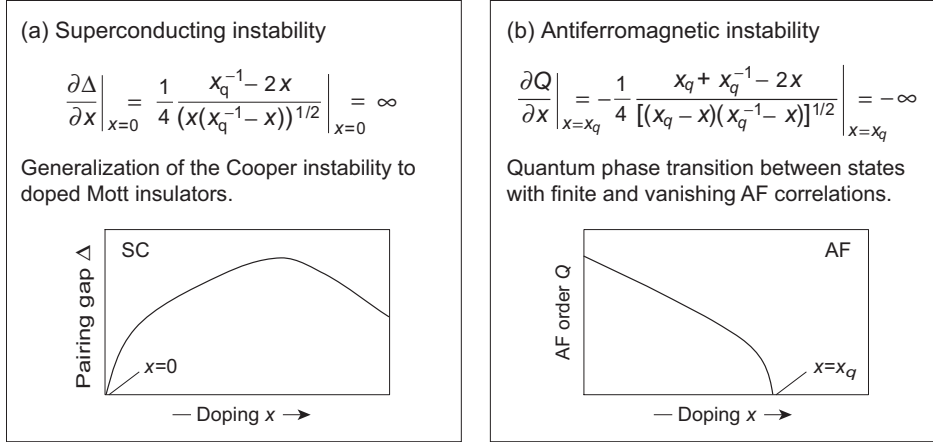


**Fig. 5.** Two fundamental SU(4) instabilities that govern the behavior of high temperature superconductors. The plots illustrate (a) the generalized Cooper instability and (b) The AF instability in terms of the values of the order parameters calculated within coherent state approximation

**Existence of a Pseudogap:** A pseudogap is a partial gap at the Fermi surface above  $T_c$ . From Fig. 4, at lower doping it is the “normal state” from which SC can be produced by lowering the temperature through the doping-dependent critical temperature  $T_c$ . As explained further below, a PG is expected from AF–SC competition in the SU(4) Hilbert subspace [11].

**Quantum Critical Behavior:** A highest symmetry with multiple dynamical symmetry subchains leads naturally to quantum phase transitions as tuning parameters such as doping, magnetic field, or pressure shift the balance between competing dynamical symmetries. The SU(4) theory is microscopic so one can determine whether these transitions are associated with critical behavior and examine the corresponding physical consequences. Thus, SU(4) and its dynamical symmetry subchains are a laboratory for quantum critical behavior in HTSC. As we now discuss, the SU(4) model implies two fundamental instabilities leading to quantum phase transitions that are central to understanding HTSC, and a *critical dynamical symmetry* that generalizes a quantum critical point to an entire *quantum critical phase*, which proves useful in understanding the underdoped region in general and the PG region in particular.

**The SU(4) Cooper Instability:** The SU(4) solution at  $T = 0$  for the pairing order parameter  $\Delta$  given in Eq. (24b) of Ref. [4] implies that [9]

$$\left. \frac{\partial \Delta}{\partial x} \right|_{x=0} = \frac{1}{4} \frac{x_q^{-1} - 2x}{(x(x_q^{-1} - x))^{1/2}} \Big|_{x=0} = \infty, \quad (1)$$

where  $x$  is doping and  $x_q$  is a critical doping value predicted by the theory. (In Fig. 4 the critical doping point is labeled  $P_q$  with  $x_q \sim 4P_q$ .) This implies a fundamental pairing instability at  $x = 0$ : the SU(4) AF Mott insulator ground state at half filling is intrinsically unstable against a QFT that condenses singlet hole pairs for infinitesimal hole doping in the presence of non-zero attractive pairing [9]. Figure 5(a) illustrates. Hence, the rapid onset of SC with hole-doping in the cuprates results from a Cooper-like instability for  $d$ -wave pairs in an AF Mott insulator. The SU(4) solution reduces to ordinary  $d$ -wave BCS theory if the AF interaction vanishes and to an AF Mott insulator if the pairing interaction vanishes [4]. Thus it generalizes the Cooper instability to doped Mott insulators and may be viewed as the traditional Cooper instability for a Fermi sea polarized by strong onsite Coulomb repulsion and AF correlations, or equivalently as a Fermi sea exhibiting SU(4) symmetry [11].

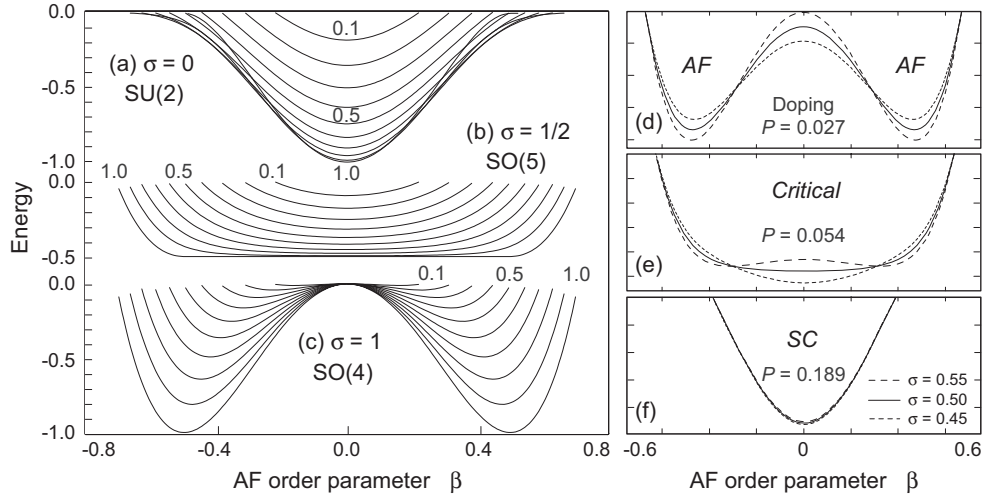


**Fig. 6.** (a-c) Coherent-state energy surfaces for symmetry limits of the SU(4) Hamiltonian [2]. The horizontal axis measures AF order. Curves are labeled by lattice occupation fractions with the value 1 corresponding to half filling. The parameter  $\sigma$  is the ratio of AF coupling to the sum of AF and pairing coupling strengths. (d-f) Effect of altering the ratio  $\sigma$  for three values of doping in the cuprates. In (d) and (f) the system is in the stable minima associated with AF and SC, respectively, and changing  $\sigma$  by 10% hardly alters the location of the energy minima, but in (e) the energy surface is critical and the perturbation can flip the nature of the ground state between SC and AF minima.

**The SU(4) AF Instability:** SU(4) symmetry implies a second fundamental instability. From the SU(4) solution for the AF order parameter  $Q$  given by Eqs. (24b, 14) of Ref. [4],

$$\left. \frac{\partial Q}{\partial x} \right|_{x=x_q} = -\frac{1}{4} \frac{x_q + x_q^{-1} - 2x}{[(x_q - x)(x_q^{-1} - x)]^{1/2}} \Big|_{x=x_q} = -\infty, \quad (2)$$

and a small change in doping causes a divergence in AF correlations near the critical doping  $x = x_q = 4P_q$  in Fig. 4 [10, 11]. Figure 5(b) illustrates. This instability is associated with a QFT between a SC state still influenced by AF correlations and a pure SC state.

**Dynamical Symmetries and Critical Behavior:** Quantum phase transitions and quantum critical points are a natural consequence of fermion dynamical symmetries, implying that quantum critical behavior is a *corollary* of unconventional superconductivity, *not a cause*. Furthermore, some dynamical symmetry solutions generalize quantum critical points to entire *quantum critical phases* exhibiting critical behavior [2, 10, 11]. The SU(4)  $\supset$  SO(5) dynamical symmetry is an example. This is seen most easily in generalized coherent state approximation [2], which represents symmetry-constrained Hartree–Fock–Bogoliubov solutions that permit SU(4) results to be expressed in terms of gap equations and quasiparticles, and that lead naturally to total energy surfaces connecting SU(4) solutions microscopically to Ginzburg–Landau theory. SU(4) coherent state energy surfaces are displayed in Fig. 6(a-c). The flat critical nature of the SO(5) surface is evident for low doping in Fig. 6(b).

**Complexity in the Underdoped Region:** As suggested in Fig. 6(d-f), the underdoped  $\sim$ SO(5) energy surface exhibits *complexity* because many potential ground states with very different order parameters have almost the same energy. Complexity implies susceptibility to fluctuations in AF and SC order induced by small perturbations and the phase defined by the SO(5) dynamical symmetry is a *critical dynamical symmetry*. Critical dynamical symmetries are a fundamental organizing principle for complexity in strongly-correlated nuclear structure and

condensed matter systems [10,11]. In Ref. [10] we have proposed that stripe and checkerboard patterns, amplification of proximity effects, and related phenomena common in underdoped compounds may be a consequence of complexity enabled by the critical nature of the energy surface there. This complexity can occur with or without associated spatial modulation of charge. Charge is not an  $SU(4)$  generator so it is not fundamental for HTSC, but it can play a secondary role by perturbing critical energy surfaces in underdoped compounds.

**Competing Order or Preformed Pairs:** In the *competing-order model* the PG is an energy scale for order competing with SC. In the rival *preformed pairs model* pairs form at higher energy with phase fluctuations that suppress long-range order until at a lower energy the pairs condense into a SC with long-range order. In  $SU(4)$  the PG scale is an AF correlation competing with SC but the AF operators are generators of  $SU(4)$  and the collective subspace is a superposition of pairs. Thus, the PG results from a superposition of  $SU(4)$  pairs that can condense into a strong superconductor only after AF fluctuations are suppressed by doping. Hence the  $SU(4)$  pseudogap state results from competing AF and SC order in a basis of fermion pairs and *SU(4) unifies the competing order and preformed pair pictures.*

**Fermi Arcs and Anisotropy of Pseudogaps:** The  $SU(4)$  cuprate model implies strong angular dependence in  $k$ -space, which leads to temperature and doping restrictions on regions of the Brillouin zone where ungapped Fermi surface can exist [8, 11]. If this region is interpreted in terms of Fermi arcs, the  $SU(4)$  model gives a natural description of arc lengths as a function of temperature in quantitative accord with ARPES data [8, 11]. If the Fermi surface is interpreted in terms of small pockets instead,  $SU(4)$  symmetry restricts their possible location and size.

**New Superconductors:** In 2004 we argued that the essence of cuprate SC is non-abelian dynamical symmetry, and that compounds with similar symmetries but different microscopic structure should exist [3]. Discovery of Fe-based SC in 2008 validated this prediction [7, 11].

**$SU(4)$  and Conventional BCS Superconductivity:** The relationship of  $SU(4)$  to BCS SC was given in Fig. 3. Conventional SC is the limit of  $SO(8) \supset SU(4)$  SC when Coulomb repulsion is small and AF correlation is negligible. Thus  $SO(8) \supset SU(4)$  dynamical symmetry provides a unified view of conventional and unconventional superconductivity [11].

**Dynamical Symmetry and Universality of Emergent States:** Dynamical symmetries for a variety of emergent states suggest an even broader unification transcending fields and sub-fields. Figure 7 shows that phase diagrams for unconventional SC emergent states in a broad range of condensed matter systems and in nuclear structure are remarkably similar, despite completely different microscopic physics (see Refs. [11, 18] for further discussion). An even more remarkable universality of emergent states is shown in the coherent state energy surfaces displayed in Fig. 8. Seemingly different emergent modes: collective states for atomic nuclei, for graphene in a magnetic field, and for cuprate high-temperature SC, give nearly identical energy surfaces under a suitable mapping of respective order parameters and rescaling of energy. Microscopically these modes differ fundamentally but they share a common Hilbert-space truncation to a collective subspace dictated by shared Lie algebras that care only about commutators of generators, not their microscopic structure [11].

## 4 Transition Temperatures for Unconventional Superconductors

The discussion above shows that  $SU(4)$  dynamical symmetry describes a broad range of cuprate SC properties using a minimum of adjustable parameters or adjustable assumptions. Having established that it should be taken seriously, let's ask what  $SU(4)$  symmetry has to say about  $T_c$ . The generators of  $SO(4)$  antiferromagnetism and  $SU(2)$  superconductivity are also generators of  $SU(4)$ . This implies that (1) AF and SC compete for the collective Hilbert subspace, and (2) AF states and SC states are related by a rotation within the  $SU(4)$  group

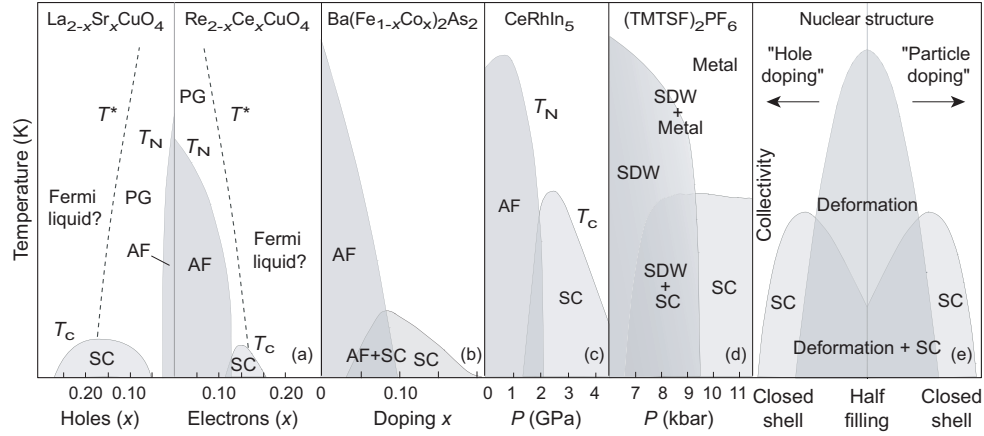


**Fig. 7.** Universality of superconductivity and superfluidity. (a) Phase diagram for hole- and electron-doped cuprates [14]. Superconducting (SC), antiferromagnetic (AF), and pseudogap (PG) regions are labeled, as are Néel ( $T_N$ ), SC critical ( $T_c$ ), and PG ( $T^*$ ) temperatures. (b) Phase diagram for Fe-based SC [15]. (c) Heavy-fermion phase diagram [16]. (d) Phase diagram for an organic superconductor (SDW denotes spin density waves) [17]. (e) Generic correlation-energy diagram for nuclear structure [18].

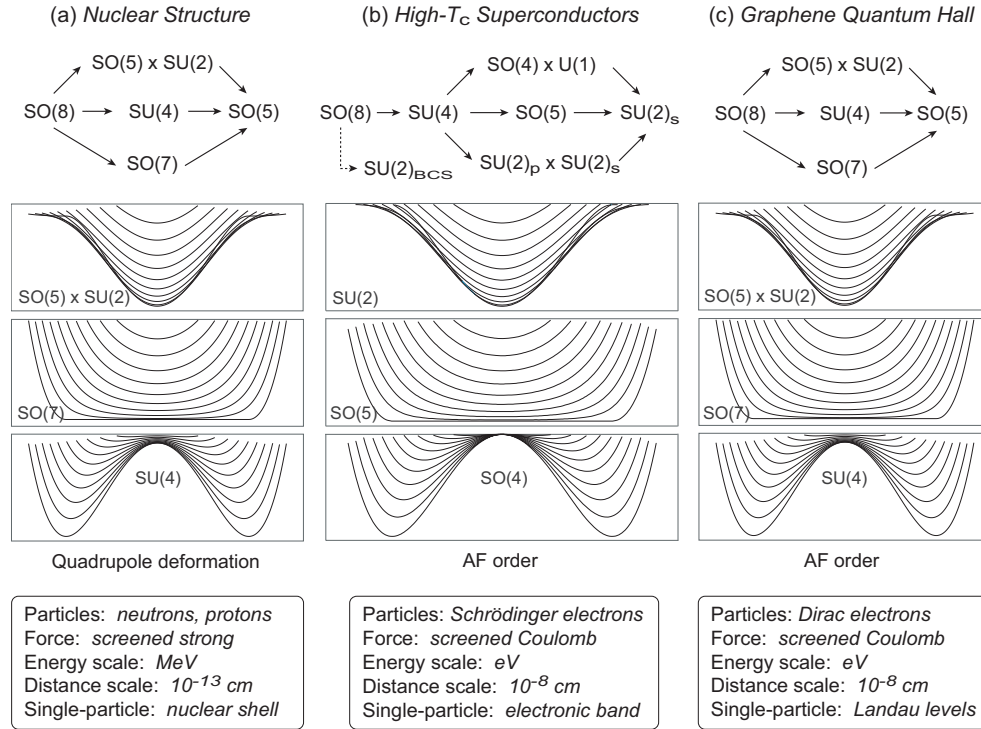


**Fig. 8.** Similarity in the dynamical symmetry chains and the ground coherent state energy surfaces for (a) dynamical symmetry in nuclear structure [19], (b) high-temperature SC [1,2], and (c) monolayer graphene in a strong magnetic field [20]. The plot contours show total energy as a function of an appropriate order parameter, with different curves corresponding to a particle number parameter.



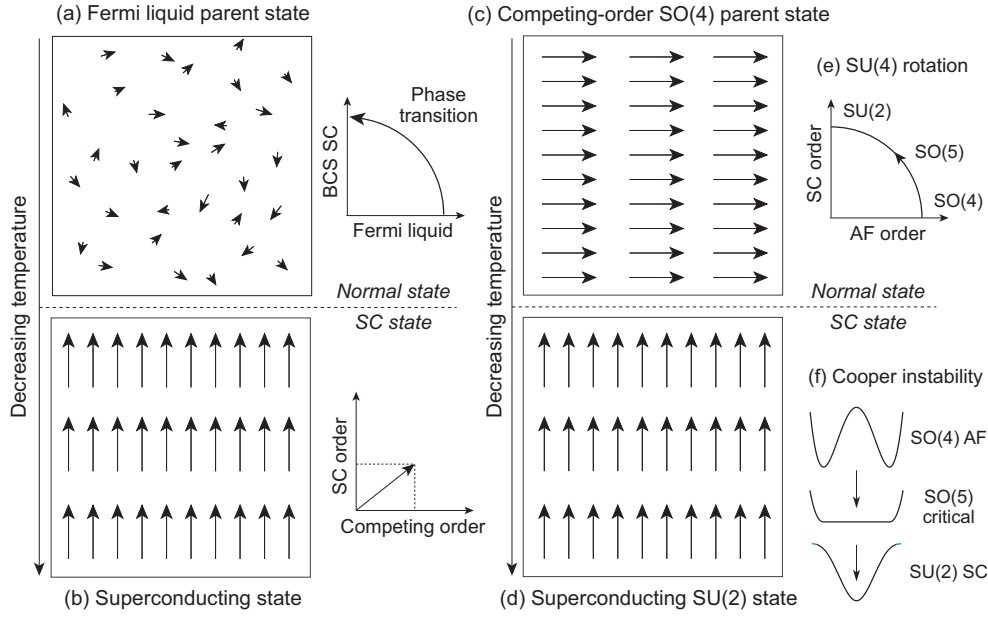


**Fig. 9.** (a)–(b) Formation of BCS superconductor by lowering the temperature of a Fermi liquid through  $T_c$ . Direction of vectors indicates relative strength of competing order ( $x$ ) and SC ( $y$ ); length indicates total  $SU(4)$  strength. The SC transition converts a high-entropy state (a) into a highly-ordered one (b), implying a low  $T_c$ . (c)–(d) Formation of SC from a parent state having order that competes with SC but is related to SC by symmetry. This requires imposing SC order (d) on a state (c) already highly ordered, which can occur at a higher  $T_c$  because it is a collective rotation in the group space between two low-entropy states. (e) Collective rotation in  $SU(4)$  group space. (f)  $SU(4)$  Cooper instability.

space. As we now explain, this implies on fundamental grounds a higher than average  $T_c$  for unconventional SC in general, and for cuprate and Fe-based HTSC in particular.

A generic reason for higher  $T_c$  in unconventional SC is illustrated in Fig. 9, where the  $x$  component of arrows may be viewed as the average competing-order matrix element squared and the  $y$  component as the average pairing matrix element squared. In the conventional BCS case of Fig. 9(a-b) there is no net SC or AF in the initial state of Fig. 9(a) and arrows are small and randomly oriented. To form the superconducting state from the parent state each arrow must be lengthened and ordered vertically in the SC phase transition, as in Fig. 9(b). This is a transition from a high-entropy initial state to a highly-ordered final state, implying that it requires a corresponding low temperature to implement. In the competing order case the initial state of Fig. 9(c) is already ordered such that a simple collective rotation can produce the SC state in Fig. 9(d). This is the general case when SC and the competing order are unified by symmetry. In essence, the collective vectors already exist as a highly-ordered configuration in the parent state with a length proportional to the  $SU(4)$  Casimir expectation value, but they point in the AF direction. To produce a superconductor from a parent AF state, they need only be rotated uniformly to point in the SC direction; Fig. 9(e) illustrates. Thus, if competing order and superconductivity are related by symmetry the parent state can “pre-condition” the phase transition, allowing it to occur at higher  $T_c$  because the low-entropy competing-order state can be rotated collectively into the low-entropy superconducting state.

We have shown that the  $SU(4)$  model exhibits a generalized Cooper instability whereby the AF Mott insulator state reorganizes spontaneously into a superconductor when it is perturbed by adding holes [9]. The collective rotation in the  $SU(4)$  space indicated in Fig. 9(c-e) is a schematic representation of this generalized Cooper instability, which can occur sponta-

neously if there is no barrier to the rotation. The  $SU(4) \supset SO(5)$  critical dynamical symmetry exhibits such a property, as illustrated in Fig. 9(f). At low doping the energy surface implies degenerate AF and SC ground states with no energy barrier between them [see Fig. 6(b) for lattice occupation fraction of one]. This suggests that the AF and SC phases can be connected by a sequence of infinitesimal  $SU(4)$  rotations through intermediate states having different mixtures of AF and SC order that are degenerate in energy.

These entropy arguments are equivalently information arguments. Figure 9(d) is obtained from Fig. 9(c) by collective rotation, which requires specification of a single angle. Conversely, there is no order in the parent state of Fig. 9(a) and each arrow must be lengthened and oriented individually to give Fig. 9(b), which requires supplying much more information. Thus the ordering necessary to condense the SC state is much larger in Figs. 9(a-b) than in Figs. 9(c-d). The information argument also makes clear the essential difference between competing collective modes that are independent and those related by a symmetry. In the former case a large amount of information is required to change the competing-order state into the SC state because they are unrelated: the symmetry of the parent state must be destroyed and the SC symmetry then constructed from the pieces. In the latter case the symmetry already encodes the relationship between the two modes; hence only a small amount of information is required to produce the SC state from the competing-order state.

Our discussion has emphasized cuprate SC examples but applies generally to unconventional SC. The crucial physics of unconventional superconductivity lies in the competition of other collective modes with pairing, and possible Coulomb repulsion effects. These polarize the pairing interaction and alter the geometry of the pairing formfactor, but that is *symptomatic*; the essential physics lies in the competing order, not the formfactor. Thus, the reason for high- $T_c$  proposed here should be operative in all unconventional SC, leading to the often abnormally high  $T_c$  (on an appropriate scale) seen for cuprates, Fe-based SC, heavy-fermion SC, and other unconventional superconductors, by virtue of universal symmetry arguments depending only parametrically on microscopic details like pairing geometry.

This work was partially supported by the National Key Program for S&T Research and Development (Grant No. 2016YFA0400501), and by LightCone Interactive LLC. L. W. acknowledges grant support from the Basque Country Government (Grant No. IT986-16), and by PGC2018-101355-B-I00 (MCIU/AEI/FEDER,UE).

## References

1. M. W. Guidry, L.-A. Wu, Y. Sun, and C.-L. Wu, Phys. Rev. **B63**, (2001) 134516
2. L.-A. Wu, M. W. Guidry, Y. Sun, and C.-L. Wu Phys. Rev. **B67**, (2003) 014515
3. M. W. Guidry, Y. Sun, and C.-L. Wu, Phys. Rev. **B70**, (2004) 184501
4. Y. Sun, M. W. Guidry, and C.-L. Wu, Phys. Rev. **B73**, (2006) 134519
5. Y. Sun, M. W. Guidry, and C.-L. Wu, Phys. Rev. **B75**, (2007) 134511
6. Y. Sun, M. W. Guidry, and C.-L. Wu, Phys. Rev. **B78**, (2008) 174524
7. M. W. Guidry, Y. Sun, and C.-L. Wu, Front. Phys. China **4**, (2009) 233
8. M. W. Guidry, Y. Sun, and C.-L. Wu, New J. Phys. **11**, (2009) 123023
9. M. W. Guidry, Y. Sun, and C.-L. Wu, Front. Phys. China, **5(2)**, (2010) 171
10. M. W. Guidry, Y. Sun, and C.-L. Wu, Chinese Science Bulletin, **56**, (2011) 367
11. M. W. Guidry, Y. Sun, L.-A. Wu, and C.-L. Wu, Front. Phys. **15**, (2020) 43301 (arXiv: 2003.07994)
12. P. Dai, et al, Science **284**, (1999) 1344
13. J. C. Campuzano, et al, Phys. Rev. Lett. **83**, (1999) 3709
14. N. P. Armitage, P. Fournier, and R. L. Greene, Rev. Mod. Phys. **82**, (2010) 2421
15. L. Fang, et al, Phys. Rev. **B80**, (2009) 140508(R)
16. G. Knebel, D. Aoki, and J. Floquet, (2009) arXiv: 0911.5223
17. K. Kang, et al, Phys. Rev. **B81**, (2010) 100509(R)
18. M. W. Guidry and Y. Sun, Front. Phys. **10**, (2015) 107404
19. C. L. Wu, D. H. Feng, and M. W. Guidry, Adv. Nuc. Phys. **21**, (1994) 227
20. L.-A. Wu and M. W. Guidry, Sci. Rep. **6**, (2016) 22423